FIRST PRINCIPLES CALCULATIONS OF TOKAMAK ENERGY TRANSPORT

M. KOTSCHENREUTHER, W. DORLAND, Q.P. LIU
Institute for Fusion Studies,
University of Texas,
Austin, Texas,
United States of America

G.W. HAMMETT, M.A. BEER, S.A. SMITH
Plasma Physics Laboratory,
Princeton University,
Princeton, New Jersey,
United States of America

A. BONDESON
Institute for Electromagnetic Theory,
Euratom–NFR/Fusion Association,
Chalmers University of Technology,
Göteborg, Sweden

S.C. COWLEY
University of California,
Los Angeles, California,
United States of America

Abstract

FIRST PRINCIPLES CALCULATIONS OF TOKAMAK ENERGY TRANSPORT.

A predictive, physics based model of tokamak energy transport that is based on simulations of the gyrokinetic equation is presented. Calculations of core energy transport are compared with experimental results from JET, TFTR, JT60-U and DIII-D for a variety of discharge conditions. In the region of the plasma predicted to be unstable to ion temperature gradient (ITG) modes (typically between the $q = 1.2$ surface and $r/a = 0.9$), the ratio of the model's prediction of the average temperature gradient scale length to the experimental value is 1.08 ± 0.17. Core H-mode temperatures are found to depend strongly on the pedestal temperature. The scaling of H-mode pedestal performance with the gyroradius parameter $\rho*$ is shown to follow from the underlying scalings of the gyrokinetic equation. An analogy is drawn between H-mode confinement and classic turbulent fluid flow in pipes which highlights the importance of the boundary layer at the edge. Experimental results on fast temperature propagation, wall effects on confinement, ELM scalings, ELM effects on confinement, confinement limits, and VH modes are qualitatively explained as natural consequences of the importance of the boundary layer. Implications of the expected $\rho*$ scaling of conventional H-mode confinement are unfavorable for ITER. Initial efforts to find a reactor relevant advanced tokamak configuration based on the idea of ITG second stability are described.

1. Introduction

To date, large energy losses have prevented the experimental demonstration of net fusion energy production from a tokamak. Here, we report that calculations based on numerical simulations of the gyrokinetic equation [1] successfully explain energy losses from the core of large tokamaks such as JET, TFTR, JT-60U and DIII-D under many (but not all) conditions. These calculations provide a scientific framework that unifies many seemingly disparate experimental phenomena and allow more realistic predictions of the performance of proposed experiments. The experimental data used to test the theory is taken from the ITER profile database [2]. L-modes, hot-ion modes and ELMy and ELM-free H-modes are included in the dataset. When full numerical equilibria were not available, an approximate magnetic geometry was used that includes the ellipticity, triangularity, axis shift, and their derivatives.

2. Basic Features of the Model

The gyrokinetic equation is the fundamental equation describing drift modes, ion temperature gradient (ITG) modes, ideal and resistive ballooning modes, tearing modes and other microinstabilities with frequencies less than the gyrofrequency. The linear gyrokinetic stability calculations presented here use algorithms that represent the velocity space dynamics of all species numerically, without analytical approximations [3]. Thus, kinetic effects are well described. The main approximations of the codes are that the modes are described by the ballooning transformation, valid for short wavelength modes, and that electromagnetic perturbations proportional to $\delta B_\parallel$ are neglected. As previously reported for TFTR L-modes [1], the ITG mode is observed to be the dominant core instability. Trapped particle instabilities are found near the edge of some discharges and in the center of hot-ion discharges. When the trapped particle modes are absent, there is a critical ion temperature gradient below which there is no predicted micro-instability.

Nonlinear toroidal gyrofluid simulations are used to parameterize the transport which results when the ITG instability boundary is crossed [4]. These high-resolution 3D simulations include the ExB nonlinearities, and linear closure approximations that describe kinetic effects. The gyrofluid simulations are carried out in the radially local, or flux-tube limit, mathematically similar to the ballooning limit. They have been linearly benchmarked with gyrokinetic codes for a wide range of parameters. Limited comparisons with nonlinear gyrokinetic particle simulations have also been carried out.

Results summarizing the performance of the model are shown in Fig. (1). The temperature gradient appears as an instability driving term in the gyrokinetic equation as the inverse scale length $R/L_T = - (R/T)\, dT/dr$. When $R/L_T > R/L_{Tc}$, the ITG mode is unstable. Note that $R/L_{Tc}(r)$ depends on local dimensionless parameters. [Unlike in Ref. [1], here we explicitly calculate R/L_{Tc} using the gyrokinetic codes at each radial point.] In Fig. (1a), the radial average of the experimental gradient to the critical gradient is shown, where the average is taken between the q=1.2 surface and r/a=0.9 for L-modes and H-modes. For non-sawtoothing hot ion modes, the inner boundary extends inward to the region where neoclassical transport becomes comparable to ITG transport. Regions in which there is no critical temperature gradient, because of the appearance of trapped electron modes, are not included in the radial average. The stabilizing effect of velocity shear is estimated using the criterion that the stabilization is linearly proportional to dv_E/dr, and complete stabilization occurs when the linear growth rate $\gamma = dv_E/dr$, as found by nonlinear simulations [5]. As can be seen, ion temperature profiles in H-mode discharges tend to be close to the marginally stable profile, whereas some L-mode discharges are well above it.

The L-mode shots are well above marginal stability toward the edge, as found on TFTR. The departure from marginality in L-modes arises because the turbulent heat flux of the ITG mode scales with temperature as $T^{5/2}$, for fixed deviation from marginal stability, so the ITG mode is not strong enough to force the profile close to marginality in a low-temperature edge. Thus, the ITG
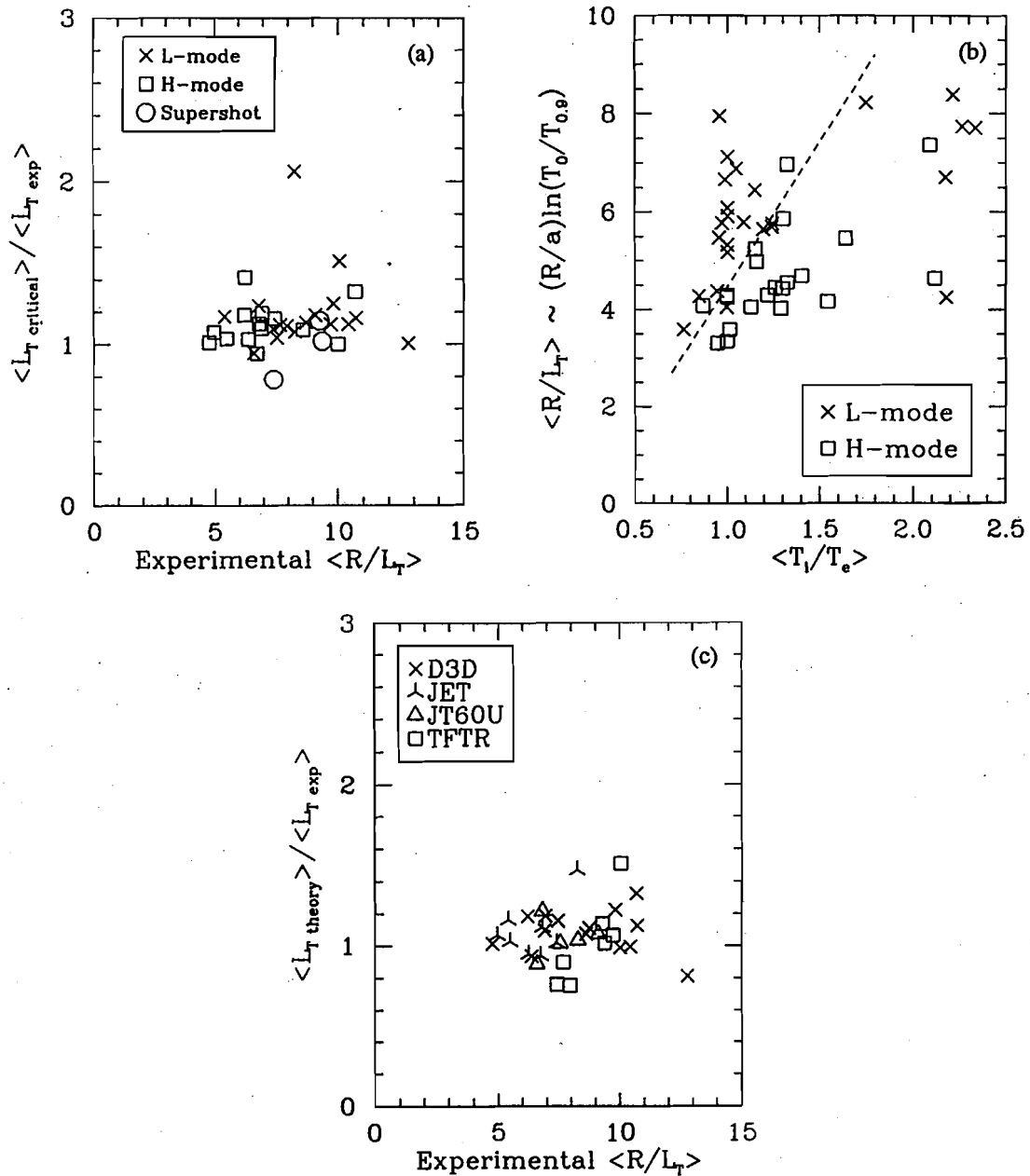
FIG. 1. Radially averaged critical scale lengths, experimental scale lengths, and predicted scale lengths including the gyrofluid χ, in the ITER profile database.

drive ($\sim R/L_T$) increases to conduct the power at low temperature. Another robust feature of ITG transport is that increasing T_i/T_e weakens the ITG mode, by increasing the critical gradient. Both of these gross features are borne out by the ITER database, in Fig 1. The $<R/L_T>$ increases with T_i/T_e, and for fixed T_i/T_e, the L-mode discharges have higher $<R/L_T>$, consistent with a stronger ITG drive and poorer confinement.

Results of nonlinear gyrofluid simulations [4] show that most of the parameter variation in the nonlinear χ from ITG modes can be captured from the linear eigenfunctions. Specifically, it is found that if one defines $W=\chi_{nonlinear}/D_{mixing}$ (where D_{mixing} is the maximum value for all k_θ of

γ/k_{perp}^2)the function W depends strongly only upon the departure from criticality and magnetic shear, and can therefore be parameterized by a modest number of nonlinear simulations [1]. Here, we combine the gyrokinetic code above (which has more complete linear physics) with the gyrofluid results by taking $\chi_{nonlinear}$= W D_{mixing}, where D_{mixing} is computed directly from the gyrokinetic code. The electron heat flux is obtained using the quasilinear ratio of electron to ion heat fluxes from the gyrokinetic code (however, the ion heat flux usually dominates) [1].

When the incremental increase in the temperature gradient beyond R/L_{Tc} is calculated using this algorithm, the average predicted $<R/L_T>$ is 1.08 times the experimental value, and the standard deviation is 0.17 (Fig. 1b). The experimental uncertainty in $<R/L_T>$ is roughly 10%. Errors in the predicted gradient which are from errors in experimental quantitites (such as Z_{eff}, q, etc.) are probably at least another 10-20%. Thus, we believe that the agreement in Fig. (1b) is within the error bars.

3. Sensitivity of Global Confinement to Pedestal Performance

The improved core confinement in H-modes follows from the edge transport barrier. For the H-mode discharges in the ITER Profile Database, we find that the predicted ion temperature profiles are within 5% of the marginal stability from the core to the top of the pedestal. In this limit, the core temperature profile is only determined to within a multiplicative constant, since multiplying T(r) by a numerical factor does not change the marginality condition on (R/T) dT/dr. This is a qualitative difference between ITG modes and the RLW model. Specification of the pedestal temperature boundary condition therefore determines the core temperature [1]. The improved confinement in supershots and hot ion modes also arises partly because of improved edge temperatures, but in addition the critical gradient becomes larger for larger Ti/T_e, and modest thermal deuterium dilution[1].

In H-mode experiments, the central temperature rapidly responds to the edge temperature [6,7]. This behavior may be understood from the model: a small deviation from near marginality near the edge leads to a large change in χ, which rapidly propagates to the core by small changes in the temperature profile. Experiments on JET have shown that the central temperature responds in a few milliseconds to edge perturbations from ELMs [6], cold pulses [7], and H to L transitions [6].
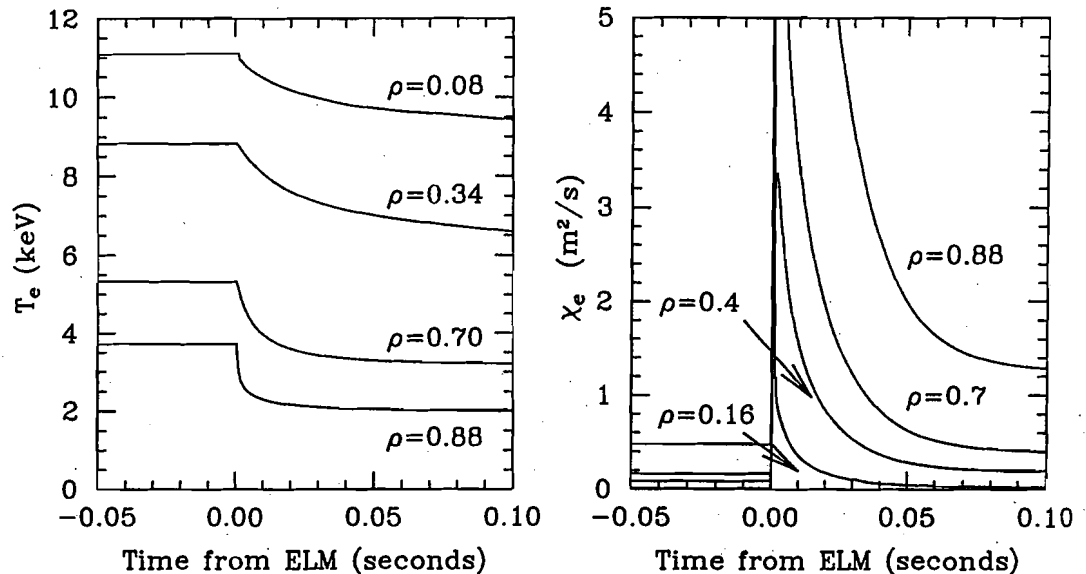

FIG. 2. Time response after a simulated ELM for electron temperature and χ_e from the ITG model.

For example, Ref. [6] reports the electron temperature response to a giant ELM for discharge #30592. Lacking data for this shot, a surrogate was chosen from the ITER database (#26087), and the effect of a giant ELM was simulated by dropping the edge boundary temperatures of all species by a factor comparable to the electron temperature drop found in Ref. [6]. The electron temperature responses in the surrogate ITG simulation [Fig (2)] are as fast as found in Ref. [6]. The electron χ is shown in Fig (2b). It can be seen that there is a rapid increase in χ_e across the discharge. Even though χ is a local function, it seems to behave non-locally. Cold pulse experiments on JET[7] have shown that the experimentally observed response is roughly consistent with a factor of eight increase in χ for roughly 5 milliseconds, similar to Fig (2b). The fact that temperature perturbations from several different sources produce similar results in the core is strong evidence for a close connection between the plasma edge temperature and the core temperature in H-modes.

4. Scaling of Pedestal Performance at Small ρ*

Unfortunately, it is not possible to predict the height of the H-mode pedestal due to the complexity of the edge physics. However, useful results can be obtained from the ρ* scalings of terms in the gyrokinetic equation, aided by insight obtained from simulations. The usual arguments for Bohm or gyroBohm global scaling assume that the scaling considerations are uniform across the minor radius. However, there is another class of solutions, in which the turbulence scales as the gyroradius in the core and is strong enough to force the profile close to marginal stability from the core to very near the edge. At the edge there is a boundary layer which scales as the gyroradius (possibly the poloidal gyroradius) where the turbulence is suppressed.

The mode (typically ITG) which is destabilized first as R/L_T is increased above R/L_{Tc} typically has $0.1 < k_\theta \rho_i < 0.6$. If the transport from the ITG mode is robust, R/L_T is forced to be close to R/L_{Tc}, and the unstable fluctuations have $k_\theta \rho_i$ of order 0.3. (Measurements in the core of TFTR show such fluctuations propagating in the ion drift direction [8].) Toward the edge of L-modes, the deviation from criticality increases and long wavelength modes become unstable. Preliminary nonlinear simulations for large values of R/L_T indicate that the ion feature in the predicted fluctuation spectrum becomes dominated by the low $k_\theta \rho$ modes, and is roughly consistent with the large spectral shift observed experimentally [8].

However, H-modes have an edge boundary layer, as does the classic description of high Reynolds number fluid flow and the turbulent flow resistance (i.e., momentum transport) in a pipe [9]. H-mode transport is fundamentally different from pipe flow, since the turbulence scale size is small for the H-mode, but is global for the pipe. However, the more crucial determinants of qualitative transport behavior are very similar: in both cases, the core turbulent dynamics only determine the core profiles to within a constant, which is found by matching to the boundary layer, causing a global sensitivity to edge conditions.

In a pipe [9], the boundary layer arises because there is a turbulence suppressing term (viscosity) in the Navier-Stokes equations which is nominally small, but which enters the equations as a higher derivative than any other term. For pipe flow, the fundamental scaling of the width of the boundary layer is found by balancing of the dominant terms in the governing equations. Gyrokinetic boundary layers form when the scale lengths of equilibrium variations become of order the wavelength of the modes, so that stabilizing terms become important. In the pedestal region, the gradients are very far above marginal stability. Nonlinear gyrofluid simulations with sharp temperature gradients of this magnitude show that an H-mode pedestal would be flattened by the turbulent transport unless the turbulent transport is suppressed by some effect not present in the lowest order of the usual ballooning ordering. We may estimate the required size of such an effect, using some insight from numerical calculations.

For parameters characteristic of H-mode pedestal well after the transition, the linear instabilities with largest growth rates are of the drift type, e.g., ITG modes and TEM (as long as the gradients

are below the MHD stability limit). The modes with the largest growth rates have $k_\theta \rho_i \sim 0.1\text{-}0.5$, and they have characteristic frequencies and growth rates of the order of ω^* ($\gamma/\omega^* \sim 1/2$ to $1/5$ is common). Within the range of gradients of interest, (*i.e.*, pressure gradients such that $a/L_p \sim 10\text{-}30$, but below the ideal MHD ballooning threshold), the growth rates are roughly linear in the gradient until the MHD limit is approached. The characteristic size of terms in the gyrokinetic equation is thus γ_0 δf, where

$$\gamma_0 = (v_{th}/L)\, k_\theta \rho_i \quad G_1(v^*, \beta, q, \varepsilon, Z_{eff}, ...)= (v_{th}/L)\, G(v^*, \beta, q, \varepsilon, Z_{eff}, ...) \tag{1}$$

Since the most unstable linear modes have $k_\theta \rho_i \sim 0.1$ and $\gamma/\omega_* \sim 1/3$, we anticipate that the typical size of G is roughly $1/30$.

In the standard ballooning limit, gradients of the E x B terms and of the driving terms are small. However, they become important in the pedestal. The widely discussed physical picture of stabilization by the sheared E x B velocity, dv_E/dr, is that velocity shear tears the perturbations apart on the same time scale as the growth of the perturbation. We note that the gradients in ω_* may have the same physical effect. Formally, the dv_E/dr term enters into the gyrokinetic equation with a size of $(dv_E/dr)k_\theta\Delta x$, where Δx is the radial correlation length. Our flux-tube nonlinear simulations find $k_\theta\Delta x$ is a function of dimensionless parameters, with no indication of an explicit ρ^* scaling. The radial electric field is estimated from the momentum balance equation in the conventional way, and the poloidal and toroidal velocities U_θ and U_ζ are taken to be of order the thermal velocity inside the layer. In the layer,

$$dv_E/dr \sim (\rho_i\, v_{th}\, /\, L^2)\, S\, (v^*, \beta, q, \varepsilon, Z_{eff}, ...) \tag{2}$$

where the leading order scaling in gyroradius is given, and typically $S \sim 1\text{-}2$. Different authors emphasize different mechanisms for the generation of U_θ, and so obtain different functional forms for S consistent with Eq. (2) (*eg.*, Shaing and Crume [10], Carreras, *et al.*, [11], *etc.*). Equation(2) also implies that the dv_E/dr term is of the same order as the term from gradients of ω_*. Note that $(1/v_{th})\, dv_E/dr \sim \rho/L^2$, whereas the other terms in the gyrokinetic equations are of order $(1/v_{th})\, \gamma_0$. As in classical fluid flow, requiring that the stabilizing terms be of order of, or larger than, the other terms in the gyrokinetic equation, we arrive at the necessary scale length of the boundary layer:

$$L < \rho_i\, (G/S). \tag{3}$$

Since we expect G/S is typically of order $1/40$, the actual width could be many gyroradii, or of order the poloidal gyroradius. If the r/R dependence and q dependence of the function G/S were r/(qR) (which is plausible for some instabilities and models for S) the width would actually scale as the poloidal gyroradius. (Similar expressions have been independently derived elsewhere [12].)

5. Experimental Evidence for Pedestal Scaling

In Table I, representative boundary layer widths for seven different tokamaks are presented, using published edge profiles and other data [3,13-18]. The major radius varies from 0.6 m to 3.1 m, the temperature from 30 eV to 1.5 keV, v^* from 0.05 to 10, and β from 0.1% to 0.7%. Even for such large parameter variation, the layer width normalized to the gyroradius only varies by a factor of 2, and by a factor of 2.6 when normalized to the poloidal gyroradius, consistent with the gyroradius or poloidal gyroradius being the fundamental scaling size.

For fluid pipe flow, wall conditions affect global confinement. Small mechanical projections that disturb the thin boundary layer (so-called "roughened pipes") reduce pipe momentum confinement time (typically by factors of two or more). The classic experimental results for this phenomenon are shown in Fig. (3): the scaling and magnitude of the pipe friction are less favorable when the width of the boundary layer is reduced to the size of the roughness scale. A qualitative analogue in

TABLE I. PEDESTAL WIDTHS FROM VARIOUS TOKAMAKS

	Width (cm)	Width/ρ_i	Width/ρ_p	Width/λ_{mfp}
JET	2.5	16	3.5	6
JT-60U	5.6	27	2.4	8
DIII-D	3.0	16	3.3	3
ASDEX-U	2.0	17	2.3	7
JFT2-M	1.0	12	1.8	8
C-Mod	1.5	30	4.7	1.3
COMPASS-D	2.0	28	4.0	2

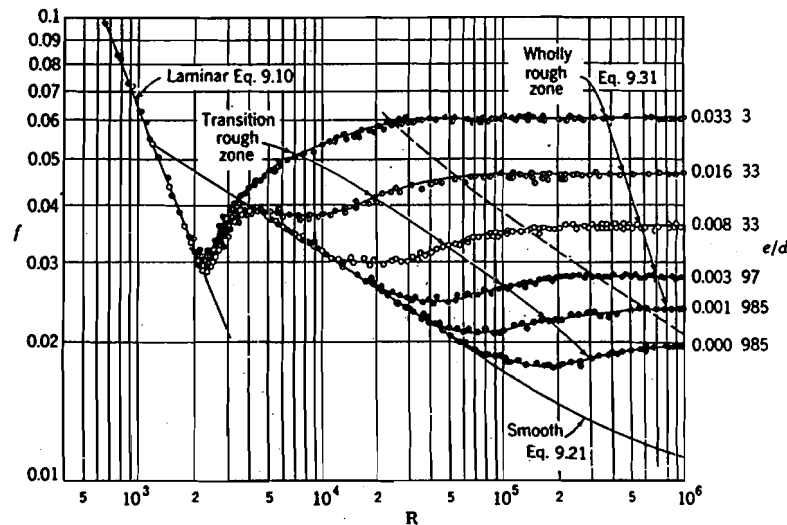*FIG. 3. Flow friction versus Reynolds number for varying wall roughness e/d. Reprinted with permission from VENARD, J.K., Elementary Fluid Mechanics, 6th edn, Wiley, New York (1982).*

H-mode physics is the observed sensitivity of confinement to wall conditioning. Atomic processes are necessarily localized to the edge. Table I includes estimates of the mean free path of Frank-Condon deuterium neutrals into the edge. Other neutral processes and impurity penetration lengths are significantly less. Gross effects of neutrals such as convective losses and radiation losses directly affect the pedestal performance. Neutral processes also strongly effect boundary plasma parameters such as Z_{eff}, gradients of Z_{eff}, η, etc. Variations in these parameters would be expected to lead to order one changes in the functions G and S, and also in neoclassical and ion orbit heat loss rates, and thereby would be expected to affect global confinement.

The linear stability of the sharp gradient region of the pedestal is considered more quantitatively for an ITER similarity discharge on DIII-D shown in Fig. (4). The linear gyrokinetic code was used with EFIT equilibria. Note that some important parameters, such as Z_{eff} and the ratio of the temperature scale length and the density scale length, η, have considerable uncertainties in this region, so these results are only approximate. As the local pressure gradient is increased (keeping these ratios constant), the ITG/TEM instabilities with $k_\theta \rho_i \sim 0.3-1.0$ become unstable and the
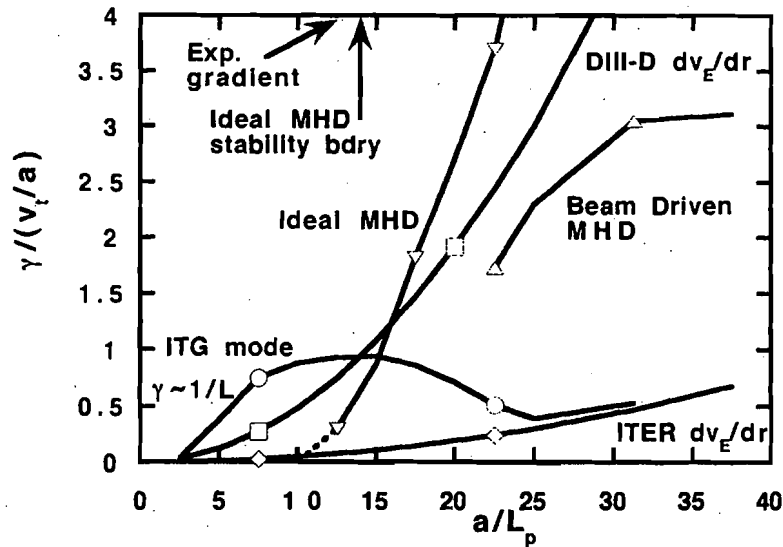
FIG. 4. Growth rates and shearing rates for the steep gradient region of the pedestal of DIII-D ITER-similar discharge 82205 at r/a = 0.97, and for the discharge scaled to ITER.

growth rates increase roughly linearly with $1/L_p$, until the ideal ballooning boundary is approached. The ITG/TEM instability growth rates then decrease, and the MHD mode at low $k_\theta\rho_i$ is dominant. Kinetic MHD modes driven by the fast particle pressure gradient also arise at $k_\theta\rho_i \sim 0.2$. Figure (4) also shows a rough approximation to the shearing rate, [Eq. (3)] with S estimated to be 1.5. For pressure scale lengths in the experimental range, the stabilizing shearing rate is of the order of the ITG growth rate, and the pressure gradient is close to the ideal MHD ballooning limit.

If the ITG/TEM modes are fully stabilized, and if other energy loss mechanisms are overcome by the heating power, the gradient will increase until the MHD limit is reached. For large dv_E/dr (i.e., large S or large $\rho*$), significant penetration into the MHD unstable region is possible. The neoclassical heat flux increases as the distance from the separatrix increases, and eventually this (along with other possible energy loss mechanisms) will pull the gradient down from the MHD limit. Even further from the separatrix, these transport processes reduce $1/L_p$ until the ITG/TEM mode is not stabilized. That is, Eq. (4) is violated, which constitutes the end of the pedestal. Thus, there may be two regions in the pedestal, one forced close to MHD limits, and another where collisional or atomic processes control the profiles.

Figure (4) also shows the estimated velocity shear after scaling this discharge to ITER. As can be seen, the linear ITG/TEM growth rates are now larger than the shearing rate. If MHD effects could be ignored, then by increasing $1/L_p$, the shearing term would eventually stabilize the ITG mode, since without the MHD effects $\gamma \sim 1/L_p$, whereas the velocity shear term increases more strongly, $dv_E/dr \sim (\rho/L_p)^2$. However, the MHD mode prevents this for β values characteristic of DIII-D. Only by decreasing the pedestal β by a factor of order $\rho*^{ITER} / \rho*^{DIII-D}$ can the velocity shear in ITER stabilize the ITG modes without first violating MHD stability.

6. H-Mode Confinement β limits

Due to ITG marginality, any process that limits the pedestal temperature can limit the attainable global confinement. On DIII-D, JT60-U, JET, and other machines, in many types of high β discharges, some fraction of the pedestal is found to be quite close to ideal MHD marginal stability for ballooning modes or kink modes. Predictive simulations with MHD stability and gyrokinetic

transport from the separatrix to the core are beyond our present capabilities. However, some qualitative explanations of physical mechanisms and scalings of important processes are presently possible.

Recent VH-mode experiments [20] provide a comparison of two cases: one where the edge is limited by MHD processes and another where the edge is second stable. When the edge is second stable, VH-modes arise and persist as long as the plasma does not experience ELMs (an indication that MHD edge stability has been lost). After an X event, the discharges revert to ELMing H-modes with half the confinement time of the preceding VH phase. Otherwise similar discharges with less triangularity (which have poorer edge MHD stability) do not enter the high confinement VH phase, but are ELMing H-modes.

Velocity shear driven by neutral beams contributes to VH-mode confinement. This is consistent with boundary effects. As the temperature at the boundary is increased at fixed heating power, the transport power needed to enforce marginality decreases. Thus, local fluctuation levels decrease, leading to a roughly proportional improvement in momentum diffusivity. The resulting increased velocity shear further improves the local effective critical gradient and provides a substantial amplification of the improved confinement from the boundary temperature increase alone. Thus, VH-modes show a correlation between global confinement improvement and improved edge MHD stability which is qualitatively consistent with the ITG model.

The parameter $\alpha = -2\mu_0 \, (q^2 R/B^2)$ dp/dr arises in ballooning stability theory in the well-known s-α model. On JT60-U, this parameter was observed to approach the value for instability before ELM events [21]. Also, the pedestal parameters were found to satisfy an empirical relationship [21], which can be written:

$$\beta(q^2 R) / \rho_{pol} = C (\kappa, \delta, l_i). \tag{4}$$

This is equivalent to the criterion that the ideal ballooning parameter (with the ion β) is at marginal stability if the pressure gradient scale length is replaced by a constant times the poloidal gyroradius [21]. This links the scaling results for the layer width in Eq. (4) to edge MHD stability limits.

The boundary layer nature of confinement in the ITG theory links ELMs to global confinement degradation, both transiently, as in Fig. (2), and also in steady state if the ELMs are frequent. JT-60U found that increased heating power resulted in progressively more frequent ELM events with progressive deterioration in the H factor [21]. Hender *et al.*,[22] found that ELM events frequently signal the end of the good performance phase of JET discharges, by substantially lowering central ion temperatures. Challis, *et al.*, [23] reported transport β limits for low-q discharges similar to ITER, which seemed linked to increased ELM activity (not magnetic islands).

The most direct evidence on JET of a transport limit related to edge ideal MHD instability is reported by Smeulders, *et al.*, [24]. A transport β limit prevented the attainment of large β_N for high magnetic field, but not for low magnetic field. For the high field shots which failed to obtain high β_N, most of the profile was well below the ideal MHD stability limit (by factors of as much as four), so core MHD was not responsible. However the edge was close to computed MHD limits, and the global confinement degradation of high field shots was attributed to observed edge MHD instabilities. According to Eq. (5), a discharge in a large machine at high field would have small ρ^* and thus MHD stability would imply lower pedestal β. For flat density profiles as observed on JET, ITG temperature marginality translate an edge β limit into a core β limit.

Balet, *et al.*, [25] report on a comparison of two ITER similarity discharges with virtually identical core temperature and density profiles, but with differing pedestal density profiles. One discharge had a steeper density profile in the boundary layer, generated by more intense gas puffing. The heating power needed to sustain this discharge was 40% higher. The degraded confinement was attributed to the increase in the frequency of ELMs.

7. Reactor Relevance of H-mode Operation

In light of this, we consider the $\rho*$ scaling of H-mode confinement for small $\rho*$. Experimental $\rho*$ scans have been described as analogues to the use of wind tunnels, where scale models are tested at Reynolds numbers different than the actual device, and projected performance parameters (*e.g.*, frictional drag) are obtained by scaling in Reynolds number. Consider the Reynolds number scaling of flow drag inside a pipe in Fig. (3). For sufficiently low viscosity, the scale size of the boundary layer shrinks sufficiently so that other physical processes determine the boundary physics, *i.e.*, when the layer shrinks to the size of the mechanical roughness of the pipe wall. The same qualitative process is to be expected for H-mode confinement: the global scaling depends on the boundary layer scaling, which itself may change as the boundary layer width shrinks and MHD effects dominate. Restating this, the assumptions needed to justify conventional $\rho*$ scaling extrapolations are inapplicable, since a crucial dimensionless parameter, the pedestal β, acquires an explicit dependence on $\rho*$ in view of Eq. (4).

The widely used expression ITER93H assumes that confinement depends on all variables in a log-linear way. However, Dorland and Kotschenreuther [26] found that variables containing estimates of $\alpha/\rho*^2$ or $\beta/\rho*^2$ from global quantities consistently show the most evidence of non-log-linear behavior in the dataset. There is a slight non-log-linear degradation of H as the global quantity $\alpha/\rho*^2$ is increased.

The discharges in the H-mode database are limited to $\alpha/\rho* < 45$. Using ITER93-H, $\alpha/\rho* = 160$ for ITER. Let us consider JET discharge #33131, an ITER H-mode demonstration discharge which exhibited an apparent transport β_N limit due to ELMs [25]. This discharge had the highest value of $\alpha/\rho*$ of all the reported JET and DIII-D ITER demonstration discharges, with $\alpha/\rho* = 33.3$. The ELMs in this discharge have been interpreted as being due to proximity to the L-H threshold, since $P_{heat}/P_{thresh} = 2$. However, other ITER similar discharges [25] had $P_{heat}/P_{thresh} = 2$, and did not show degraded degraded confinement. Furthermore, in 33131, the ELM frequency decreased by a factor of two as the heating power was stepped down by a factor of two. This proportionality is consistent with profiles near the $\alpha/\rho*$ limit.

Since the functional form of the confinement degradation with $\alpha/\rho*$ is not known, and there is no statistical data for relevant $\alpha/\rho*$, we use the following reasoning. Analysis by the ITER JCT [27] supports the argument that the edge pressure gradients are limited by MHD ballooning modes over a distance of several ρ_{pol} (and proposes this as a possible physical mechanism for the Greenwald limit, when MARFE's are also included). An expression similar to Eq. (4) is obtained. Since $\rho*$ is about 5--10 times smaller on ITER than on present machines, Eq. (4) implies a severely limited pedestal β. To ameliorate this, we use a larger value of C, which is consistent with strong plasma shaping [21]. To examine ITER, we take the density profile to be flat from the pedestal inward and use Eq. (4) for the boundary temperature. Using the ITG model in a predictive transport code with ITER base case parameters, and depending upon details of the current and density profiles, the energy confinement time is roughly 2.4 seconds, or $\tau \sim \tau_{ITER89-P}$.

This implication of the limitation of the pedestal pressure on global confinement follows from empirical evidence as well. ITER requires a central temperature of roughly 15 keV. If the boundary temperature is limited to 300 eV, then the required ratio of the central temperature to the pedestal temperature is 50. This ratio is simply related to the radial average of $<R/L_T>$ over this region, and this would be 12 for ITER. Experimentally obtained values of $<R/L_T>$ (from the ITER profile database) are shown in Fig. (1). Higher values of $<R/L_T>$ are found in L-mode plasmas, with higher transport losses, consistent with the ITG model. For $T_i/T_e \sim 1$, ITER would therefore be expected operate deep in the L-mode confinement regime, or in H-mode, with substantially lower central temperatures.

Confinement performance at the L-mode level in ITER would result in Q ~1. This may seem paradoxical, since present machines which are much smaller than ITER are anticipated to achieve Q close to one in high confinement operating modes. This demonstrates that the confinement improvement obtained by taking advantage of favorable parametric dependences of the mechanism causing transport can easily outweigh the confinement advantage of larger size. We thus turn to advanced confinement modes which have been found on TFTR [28], DIII-D [29], and other tokamaks with reversed central shear.

8. Advanced Confinement

Several analyses of TFTR and DIII-D reversed shear discharges have been carried out by ourselves and others in the community. The strong confinement enhancement found in reversed shear discharges is generally found to derive in large part from shear flow stabilization, with assistance from low local magnetic shear to reduce the growth rate. Our further local shear analysis of TFTR discharges shows that typical levels of reversed global shear reduce growth rates only slightly, and that the main contributor to the local shear reversal is from the large Shafranov shift. Because shear flow stabilization has an explicit unfavorable $\rho*$ scaling, one is forced to consider geometries with larger Shafranov shifts to take advantage of "second stability" regimes for ITG/TEM modes.

Maximization of the stabilizing effect of Shafranov shift leads one to consider oblate, reverse triangularity plasmas, with elongation less than unity (inward pointing triangle). There are many potential advantages to this configuration. However, their MHD stability properties are generally regarded to be poor. We have therefore begun a series of profile optimization studies using the MARS and CHEASE codes [30], in conjunction with the gyrokinetic stability codes, to look for self-consistent (transport and MHD) profiles with favorable second stability properties. For $\kappa = 0.6$, $\delta = -0.5$, $R/a = 2$, and with an ideal wall between $r/a = 1.05$ and 1.2, we have found profiles stable to MHD ballooning and n=1 kink modes at $<\beta*> = 3.9\%$ and $\beta_N = 4.9$. Preliminary microinstability calculations find that pressure profiles with this range of $<\beta*>$ may be in the second microstability regime for ITG/TEM modes. However, we must upgrade our gyrokinetic codes to describe electromagnetic perturbations proportional to $\delta B_\parallel$ before reaching this conclusion.

In more conventional geometries, VH-mode plasmas find MHD second stability in the plasma edge for strongly shaped, high poloidal β, and appropriate edge current values [Huysmans]. We find that profiles qualitatively consistent with these MHD stability results, which are deeply into the MHD second stable regime, are very close to ITG/TEM second stability, with growth rates so low that velocity shear effects at the stongly reduced levels of a reactor are still sufficient for stabilization. Thus, with edge current profile control, a reactor relevant mode similar to a VH-mode may be possible with sharply reduced velocity shear.

REFERENCES

[1] KOTSCHENREUTHER, M., DORLAND, W., BEER, M.A., HAMMETT, G.W., Phys. Plasmas 2 (1995) 2381;
DORLAND, W., et al., in Plasma Physics and Controlled Nuclear Fusion Research 1994 (Proc. 15th Int. Conf. Seville, 1994), Vol. 3, IAEA, Vienna (1996) 463.
[2] CONNOR, J.W., et al., IAEA-CN-64/FP-21, this volume.
[3] KOTSCHENREUTHER, M., et al., Comput. Phys. Commun. 88 (1995) 128.
[4] BEER, M.A., HAMMETT, G.W., Phys. Plasmas 3 (1996).
BEER, M.A., et al., Phys. Plasmas 2 (1995) 2687;
WALTZ, R.E., et al., Phys. Fluids B 4 (1992) 3138.
[5] WALTZ, R.E., et al., Phys. Plasmas 1 (1994) 2229.
[6] PARAIL, V.V., et al., in Plasma Physics and Controlled Nuclear Fusion Research 1994 (Proc. 15th Int. Conf. Seville, 1994), Vol. 1, IAEA, Vienna (1995) 255.

[7]   DE ANGELIS, R., et al., in Controlled Fusion and Plasma Physics (Proc. 22nd Eur. Conf. Bournemouth, 1995), Vol. 19C, European Physical Society, Geneva (1995) I-053.

[8]   DURST, R., et al., Phys. Rev. Lett. 71 (1993) 3135.

[9]   Introductory fluid mechanics texts usually describe this; see, for example, VENARD, J.K., Elementary Fluid Mechanics, 6th edn, Wiley, New York (1982) 357–387.

[10] SHAING, K.C., CRUME, E.C., Jr., Phys. Rev. Lett. 63 (1989) 2369.

[11] CARRERAS, B.A., et al., Phys. Plasmas 1 (1994) 4014.

[12] CORDEY, J.G., et al., Plasma Phys. Control. Fusion 37 (1995) 773;
      CHERUBINI, A., et al., in Proc. H-mode Workshop, Plasma Phys. Control. Fusion (1995).

[13] WEISEN, H., et al., Nucl. Fusion 31 (1991) 2247.

[14] HAWKES, N.C., et al., Plasma Phys. Control. Fusion 38 (1996) 1261.

[15] SNIPES, J.A., et al., Plasma Phys. Control. Fusion 38 (1996) 1127.

[16] IDA, K., HIDEKUMA, S., Phys. Rev. Lett. 65 (1990) 1364.

[17] SUTTROP, W., et al., in Controlled Fusion and Plasma Physics (Proc. 22nd Eur. Conf. Bournemouth, 1995), Vol. 19C, European Physical Society, Geneva (1995) III-237.

[18] CAROLAN, P.G., et al., ibid., p. II-133.

[19] HATAE, T., et al., in Rep. 96-018, Japan Atomic Energy Research Inst., Ibaraki (1996) 68.

[20] OSBORNE, T.H., et al., Nucl. Fusion 35 (1995) 23.

[21] KAMADA, Y., et al., Plasma Phys. Control. Fusion 36 (1994) A123.

[22] HENDER, T.C., et al., in Controlled Fusion and Plasma Physics (Proc. 22nd Eur. Conf. Bournemouth, 1995), Vol. 19C, European Physical Society, Geneva (1995) II-029.

[23] CHALLIS, C.D., et al., ibid., p. II-069.

[24] SMEULDERS, P., et al., ibid., p. IV-061.

[25] BALET, B., et al., in Controlled Fusion and Plasma Physics (Proc. 23rd Eur. Conf. Kiev, 1996), Vol. 20C, European Physical Society, Geneva (1996).

[26] DORLAND, W., KOTSCHENREUTHER, M., ITER Expert Group Minutes, Oct. 1995.

[27] PERKINS, F.W., et al., IAEA-CN-64/FP-24, this volume.

[28] LEVINTON, F.M., et al., Phys. Rev. Lett. 75 (1995) 4417.

[29] LAZARUS, E.A., et al., these Proceedings, Vol. 1, p. 199.

[30] LUTJENS, H., BONDESON, A., SAUTER, O., Comput. Phys. Commun. 97 (1996) 219;
      BONDESON, A., et al., Phys. Fluids B 4 (1992) 1889.

[31] HUYSMANS, G.T.A., et al., in Controlled Fusion and Plasma Physics (Proc. 22nd Eur. Conf. Bournemouth, 1995), Vol. 19C, European Physical Society, Geneva (1995) I-201.

DISCUSSION

K. LACKNER: While I can imagine that your explanation for the fast, 'non-local' response of core transport to edge cooling would hold, through a wave of 'criticality' propagating inwards, I see a difficulty in explaining the fast improvement in the core observed on JET following an L–H transition. If the L mode is indeed substantially in the overcritical regime, the plasma should react as it would to a normal heat wave on a diffusive time-scale.

M. KOTSCHENREUTHER: The L mode plasmas are frequently close to criticality till quite near to the boundary. Thus the temperature pulse has to diffuse only a short distance before criticality propagates the perturbation rapidly to the centre. Therefore the centre still responds much faster than the global confinement time.

P.H. DIAMOND: Since you have opened the Pandora's box of the cold pulse, can you explain the remarkable result of K. Gentle that an edge cold pulse heats the centre? Keep in mind that the time-scale is the easy part — predicting $\Delta T(0)$ is the essence of the problem.

M. KOTSCHENREUTHER: Those experiments are done in ohmic plasmas with $Z_{eff} = 4$. We have not parametrized the transport for such cases. However, since a cold pulse can change T_i/T_e in such a way as to cause stabilization, such a result might be explainable.

V. PARAIL: I wonder if your model can explain the experimentally observed very slow propagation of the sawtooth crash heat pulse.

M. KOTSCHENREUTHER: If the temperature diffusion equation is linearized for a critical gradient χ, the resulting equation for small temperature perturbations has a large diffusivity and also a pinch. The pinch is of the order of the diffusivity for global perturbations. Thus I would expect sawtooth pulse propagation to be significantly slower, but we have not yet simulated this.

L.J. PERKINS: Global scaling relations show that tokamak energy confinement improves with current, elongation, etc. Do these dependences arise principally from the core values of the critical temperature gradient or from values of the pedestal?

M. KOTSCHENREUTHER: The main parameter dependence of the critical gradient is T_i/T_e. To the extent that this is held constant, most of the global confinement variation comes from the edge.

J.D. CALLEN: What would be the key phenomenology that experimentalists should look for in order to see if your ∇T_i based model is relevant to the experimentally observed 'non-local' (rapid inward) transport response from edge cooling or L–H transitions? In particular, would your model imply that the interior local fluctuation level should change rapidly and significantly, and that this causes the rapid change in the transport coefficient in the plasma interior?

M. KOTSCHENREUTHER: Yes, this certainly should happen. In addition, one might try a perturbation experiment where an impurity pellet is injected into the edge. By modifying the Z_{eff} profile, ITG critical gradients can be affected in a way which is unique to the model.